Acoustic Method for Detection Large Pneumothoraxes in the Out-of-Hospital Environment

by

Andrew J. Motz

Submitted to the
Department of Mechanical Engineering
in Partial Fulfillment of the Requirements for the Degrees of

BACHELOR OF SCIENCE IN MECHANICAL ENGINEERING

at the

MASSACHUSETTS INSTITUTE OF TECHNOLOGY

June 2023

© 2023 Andrew Motz

Authored by: Andrew J Motz
Departments of Mechanical Engineering
June 1, 2023

Certified by: Nevan Hanumara
Research Scientist, Department of Mechanical Engineering
Theis Supervisor

Accepted by: Kenneth Kamrin
Associate Professor of Mechanical Engineering
Undergraduate Officer

Acoustic Method for Detection Large Pneumothoraxes in the Out-of-Hospital Environment

by

Andrew J. Motz

Submitted to the Department of Mechanical Engineering
On June 1, 2023 in Partial Fulfillment of the
Requirements for the Degrees of

BACHELOR OF SCIENCE IN MECHANICAL ENGINEERING

Abstract

Pneumothoraxes and hemothoraxes present a medical emergency that can easily be life threatening. However, improper and unnecessarily aggressive treatment is not uncommon and poses significant risk to patients. Much of this is a result of poor diagnostic aids to assist in the detection of pneumothoraxes out-of-hospital, such as by Emergency Medical Service (EMS) providers. A simple, portable, and accurate method of clinically detecting a pneumothorax would increase the quality of patient care in austere environments. We propose to evaluate the acoustic transfer function of the human thorax for signs that a pocket of air or blood has accumulated within the pleural space. In an attempt to validate this hypothesis, we constructed a phantom model of the human thorax with artificial lungs and pleural spaces capable of being inflated with variable sized air pockets to displace the lungs. The model was subjected to a known acoustic input in the form of a frequency sweep and a low frequency square wave and the output signal was recorded at multiple points on the phantom. Analysis of four characteristics of the output revealed no discernable correlation to the volume or location of a pneumothorax. While the initial attempt to verify the hypothesis was unsuccessful, the theory remains intact. Future work to further this hypothesis could include improving the mathematical model and/or creating a higher fidelity phantom model for experimentation.

Thesis supervisor: Nevan Hanumara
Title: Research Scientist, Department of Mechanical Engineering

Acknowledgements

       I would like to thank the entire Spring 2022 2.750 teaching staff: Ellen Roche, Gio Traverso, Anthony Pennes, and many others, but especially my mentor and thesis supervisor Nevan Hanumara. I would also be remiss without thanking the other members of Team Pneumo: Jonathan Tagoe, Qiyun Gao, Sam Ingersoll, and Stacy Godfreey-Igwe, who collectively brought this project together.

       I also like to thank my EMS colleagues and mentors for the knowledge, inspiration, background, opportunities, and support they have given me over the last four years in addition to their unwavering dedication to help others in need. Lastly, to all my friends and family, none of this would have been possible without you by my side.

Table of Contents

List of Figures

List of Tables

1. Introduction

The human lungs are made of spongy tissue which inflates with inhaled air and allow for gaseous exchange of oxygen, carbon dioxide, and other trace molecules. The tissue of the lung is housed within the pleural cavity and is flush with the walls of the pleural cavity, sliding easily on inhale and exhale, lubricated by a thin layer of fluid. The gapless interface between the lung tissue and the wall of the pleural cavity is essential for effective respiratory action, since natural inhalation is driven by an internal negative pressure within the pleural cavity caused by the contraction of the diaphragm. The development of space between the lung and the wall of the pleural cavity is a serious medical condition and can be fatal in extreme cases.

When air enters the pleural space, it is called a pneumothorax, or colloquially, a "collapsed lung", and can be classified by the severity. In simple pneumothoraxes, often a small air bubble is formed spontaneously, causing the individual discomfort and potentially shortness of breath. In more severe cases, the air bubble can compromise the ability of the impacted lung to draw in air and require supplemental oxygen to assist respiration. While less common than pneumothoraxes, hemothoraxes occur when blood accumulates in the pleural space. Similarly to pneumothoraxes, hemothoraxes also displace the lung and can compromise respiratory function [1]. The most severe hemo/pneumothoraxes are classified as tension hemo/pneumothoraxes. In these extreme cases, the accumulation of air or fluid within the pleural space increases to the point that the lung is completely unable to function and the resulting pressure build up starts impacting the heart. This increased pressure can disrupt blood flow to the entire body and is fatal if not corrected within a span of a few minutes [2]. It is estimated that tension pneumothoraxes are present in up to 30% of major trauma cases[3,4].
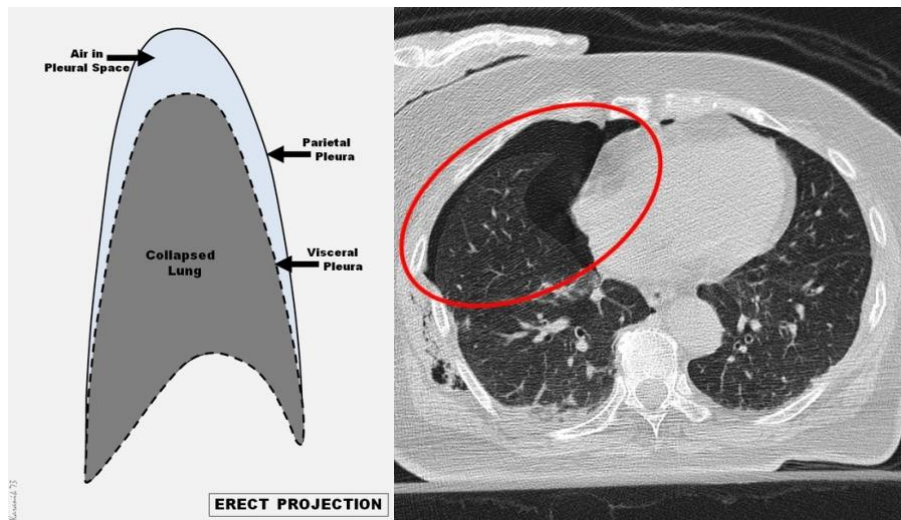
Figure 1-1: (left) Diagram of a pneumothorax. (right) CT scan from the head down showing a left sided simple pneumothorax. The dark area circled in red shows the air bubble formed between the lung tissue and the pleural wall. Note the right side does not have any dark space as the lung is flush with the wall. [5]

For simple pneumothoraxes, most patients experience recovery without any invasive medical procedures. For more severe hemo/pneumothoraxes, medical providers will place a chest line to vent the pleural cavity of excess air or fluid[1,6]. While fairly standard, this procedure is invasive and includes potential complications and lengthy recovery times. The most severe cases, where the patient faces an immediate life threat, necessitate immediate action. Emergency decompression is performed with a needle thoracostomy at predetermined locations. A hollow needle is used to pierce the skin, muscle, and pleural wall to allow trapped air or blood to escape. When performed correctly, this procedure relieves the pressure on the heart and restores blood flow to the body [2]. Whenever performed however, whether necessary or not, this invasive procedure almost certainly guarantees that a minor pneumothorax will be created requiring the patient to receive a chest tube and poses further risk of hemorrhage and cardiac injury if performed incorrectly [2–4].
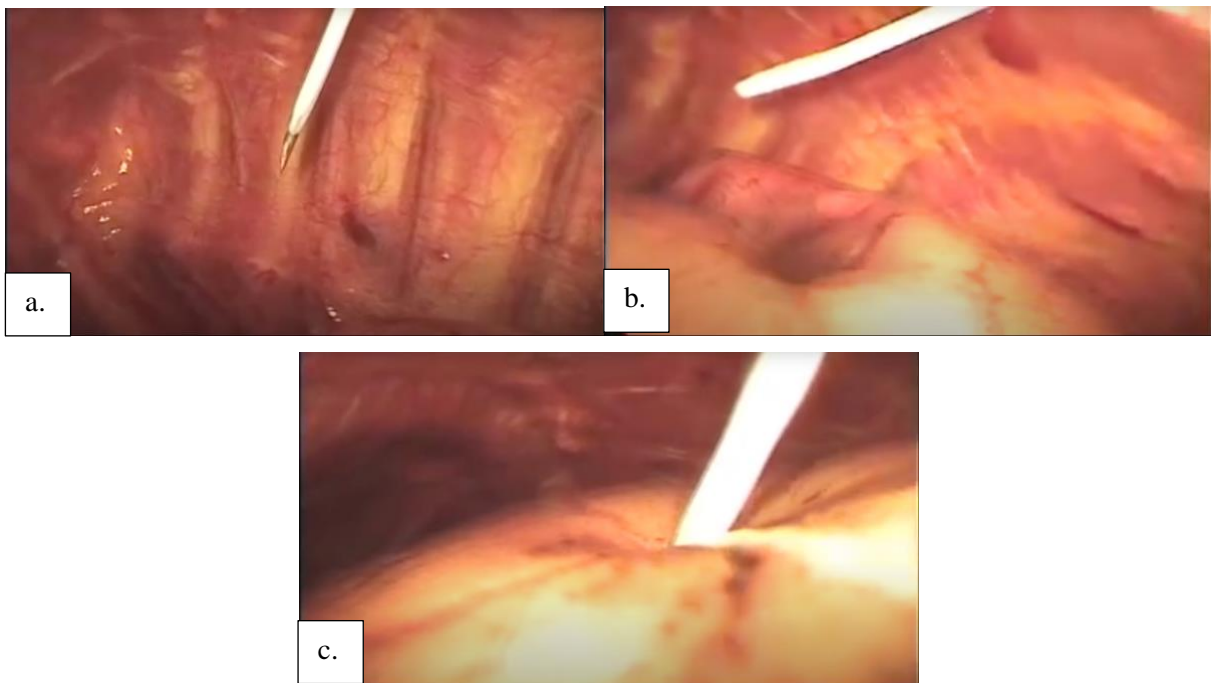
Figure 1-2: Screen captures from a thoracoscope video of a needle decompression of a tension pneumothorax. (clockwise from top left) a) The needle is inserted into the pressurized thoracic cavity. The lung is completely deflated due to the pressure. b) As air is vented through the needle the lung starts

to expand and regain functionality. c) The pneumothorax has been greatly reduced and the lung has returned to almost normal size. [7]

Medical providers currently use a host of methods to determine the presences of a hemo/pneumothorax depending on the severity. Clinical observations and risk factors are considered in concert with symptom presentation and often paired with diagnostic imaging. X-ray, Computed Tomography (CT), Magnetic Resonance Imaging (MRI), and ultrasound are commonly used and highly specific when used by a trained provider [5]. However, these methods require expensive equipment and specialized training. While widely available in American hospitals and emergency rooms, there are still many cases where it is not feasible to provide diagnostic imaging to patients. For example, in third world countries, there may not be the support services available to maintain a complicated machine like a CT scanner. Additionally, within the prehospital environment, Emergency Medical Service (EMS) providers often must make life saving decisions in austere environments with only the supplies they can carry on their backs. Without advanced imaging technology, EMS providers use basic vital signs, visual assessments, stethoscopes, and clinical intuition to determine the need for life-saving interventions [8].

Faced with limited information, EMS providers are trained to aggressively treat trauma patients who are suspected of traumatic injuries including hemo- and pneumothorax. Following this approach, many major trauma patients receive needle decompressions regardless of any specific examination for a hemo/pneumothorax. Aimed at saving lives by reducing the likelihood of a poor outcome due to a missed hemo/pneumothorax, the bar for intervention is low. High quality data is not available for the proper use of prehospital needle decompression. However, some studies have shown that ~20%, likely higher, of needle decompression that were clinically unnecessary [9]. These extra procedures introduce unnecessary risk to patients and can increase length of hospital stays.

Hence, there exists an opportunity to introduce novel methods of diagnosing hemo/pneumothoraxes. The method must be reliable, compact and portable, and accurately determine the presence of a large hemo/pneumothorax. By exploring the transfer function response of the human body as a function of volume of pneumothorax, we aim to non-invasively determine pneumothoraxes using acoustics. Whether aimed at prehospital providers, developing nations, or overburdened hospital staff, the novel method explored in this paper would benefit numerous patients and providers.

8

2. Theory

2.1 Input-Output Analysis

Current diagnostic methods rely on imaging to determine the presence of air or fluid within the pleural space. X-ray, CT, and ultrasound focus on individual points within the patient and build a comprehensive picture of the patient's medical condition with a high degree of detail and resolution. However, very few methods consider the entirety of the patient's torso as a single entity whose properties change with the introduction of a large air or fluid cavity. In other fields, significant and useful metrics are quickly learned about the physical state of materials by looking at an input output response.

Using the output of a system generated by a known input is a tried-and-true method of engineering analysis. Anecdotally, railway wheeltappers were some of the original widespread users of this method. Established in 1848 after the Versailles railway disaster, wheeltappers used a rudimentary method of listening for changes in the sound produced when hitting train wheels with a metal hammer [10]. Despite its simplicity, this method was highly effective and promoted safety within early railways. Almost two centuries later, similar methods of analysis form one of the cornerstones of Non-Destructive Testing (NDT) methods used throughout countless industries and academic fields.

A common form of NDT is Acoustic Resonance Testing (ART). ART capitalizes on the distinct characteristics of physical objects and the resulting characteristic frequencies resulting from properties such as size, shape, integrity, and density [11]. Frequently used in production quality assurance, ART generates data sets that can be compared to reference values to reveal anomalies that would indicate defects within a material.
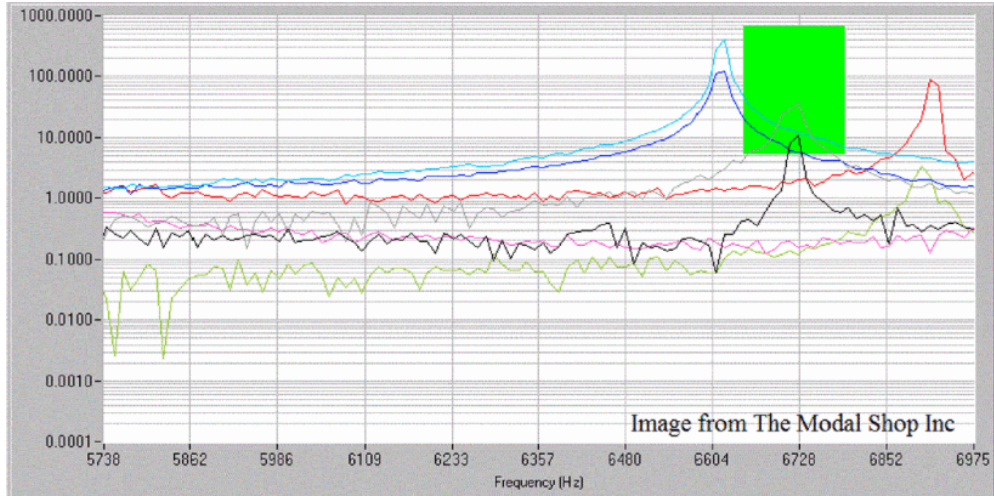
Figure 2-1: Data from an ART sample showing performance outside of standard (the green box) resulting from cracks. The resonant peaks of the sample have been shifted by the deformations. [12]

While ART is often used on traditional manufacturing materials such as metals, polymers, and concrete, it can also be used in novel applications such as evaluating the health of produce. In a study of seedless watermelons, the presence of internal voids was detected and classified with 80% success using acoustic impulse response [13]. Microphones recorded the vibrational response of a watermelon and modal analysis was performed, comparing the recorded vibration to various mathematical vibration models. Resonant frequency and band magnitude were used to determine the presence of internal hollows of varying shape [14].

Due to its non-destructive properties, limited requirements for equipment or advanced technical knowledge, and relative accuracy, ART could be applied to the field detection of pneumothoraxes.

2.2 Resonance

All physical objects experience deformation and vibration when subjected to impulses. These vibrations and specific excitations have characteristic frequencies that are stronger and more noticeable as a result of material properties and geometry. Modeling the microscopic deformation of solid objects as a damped spring-mass system, a basic single degree of freedom expression can be derived:

$$M\ddot{X}(t) + C\dot{X}(t) + KX(t) = F(t)$$

10

where M is the effective mass of the system, C is the linear damping coefficient, K is the stiffness, and F is the applied force. Solving the eigenvalue problem, the undamped natural frequency can be determined as:

$$\omega_{natural} = \sqrt{\frac{K}{M}}$$

The natural frequency is a product of the physical characteristics of the object. However, this simplified model does not easily extrapolate to the more complicated case of an air bubble developed inside a patient's chest. Introduction of a large, pressurized cavity of fluid or air within the thoracic cavity intuitively should change the output response since the pneumothorax has significantly different physical properties than a healthy lung.

A healthy lung is made up of small alveolar sacs within the spongy lung tissues. Simplifying the case to a series of bubbles within a body of dense fluid, the resonance could be calculated using the resonance equations for a Minaert bubble. Simplifying to the case of spherical bubbles in a liquid, the natural frequency of the lung tissue would be:

$$\omega = \frac{v_b}{R}\sqrt{3\delta} - i\frac{3v_b{}^2\delta}{2Rv} \text{ [15]}$$

Where $\delta = \frac{\rho_b}{\rho}$, $v = \sqrt{\frac{k}{\rho}}$, $v_b = \sqrt{\frac{k_b}{\rho_b}}$, and R is the radius of the bubble. ρ and k are the density and modulus of the outside and ρ_b and k_b is the density of the gas inside the bubble. Once the lung is collapsed and replaced with one large air bubble, the pneumothorax itself would become the "bubble" with a significantly larger radius. The larger radius would be expected to drop the resonant frequency for the fundamental resonant frequency of the thoracic cavity. This model however continues to ignore the non-uniformities within a thoracic cavity and assumes any tissue behaves similarly acoustically to a fluid.

Another potentially helpful mathematical model is that of a Helmholtz resonator. Using the natural "springiness" of air, any enclosed volume will have a resonant frequency. Basic Helmholtz frequency can be found with the equation

$$f_H = \frac{v_{air}}{2\pi}\sqrt{\frac{A}{V * L_{eff}}}$$

Where A is the area of the opening to the resonator, L is the effective length of the "neck" of the resonator, v is the speed of sound, and V is the volume of the resonator. Thus, modeling a pneumothorax as a Helmholtz resonator within the thoracic cavity would produce a decrease in resonant frequency with an increasing size of pneumothorax.

Expanding to the case of a hemothorax, when blood leaks into the pleural cavity to form a high-density fluid bubble where there would normally be spongy tissue, the bubble density and system mass would increase. From the initial simplified harmonic oscillator equation, the increase in mass of the total system should again decrease the natural resonant frequency and be detectable through basic signal analysis.

3. Experimentation

We propose to extrapolate and modify the methods used in the ART analysis of fruit health to the medical field of pneumothorax detection and explore an experimental design to validate the theoretical principles. Hemothoraxes are rarer and thus we focused on detection of a life-threatening tension pneumothorax. Since tension pneumothoraxes are clinical emergencies, testing was limited to healthy humans for baseline validation and artificial models designed to repeatably replicate emergency conditions. Thus, the establishment of an accurate phantom was necessary.

3.1 The Phantom

In order to accurately model the acoustic effects of a pneumothorax, the phantom needed to match the appropriate physical properties of the human thorax. Of most importance were the densities of the materials involved, the approximate geometries and volumes, and the ability to control the presence and size of a positive pressure bubble within the system. Our phantom was produced around a plastic rib cage to provide structure and ensure approximate anatomic geometry was followed. For simplicity, the rest of the model was molded out of a mix of Smooth-On Dragon Skin FX Pro and EcoFlex 20 silicone rubber compounds, a common flesh analog used in special effects and modeling. Two independent cavities were formed for the insertion of a phantom lung. The density of the human lung has been found to be between 0.25-0.37 g/cm^3 in healthy adults [16]. To accurately capture the spongy nature of the alveolar sacs throughout the lung, open cell acoustic foam was chosen to represent healthy lung tissue and

was wetted to better reflect the density and consistency of the lung. To simulate an air bubble developing, a two-liter anesthesia bag was placed anterior to the phantom lungs before the system was sealed in the silicon thorax. These bags allowed each side of the model to independently develop up to a 2L pneumothorax, which roughly matches the lung capacity of a small individual.

Figure 3-1: (clockwise from top left) a) The plastic skeleton model and chest mold used to cast the EcoFlex and Dragon Skin silicone rubbers. b) The completed phantom mold with internal pleural cavities included. c) The damp acoustic foam used to simulate lung tissue. d) The phantom with one complete lung, showing the anesthesia bag to be inserted into the second pleural cavity to allow for inflation of a pneumothorax.

13

3.2 Signal Generation and Data Collection

Benchtop testing determined that frequency sweeps and low frequency step inputs produced the most distinct outputs that would allow for analysis. A 4Ω/25W contact speaker was placed on the upper sternum, centered on the midline just above the nipple line. The speaker was driven by a LG CM4550 stereo and produced a MATLAB generated 20-second-long 20–2000 Hz frequency sweep and a 1 Hz square wave with 50% duty cycle. Audacity collected the output files from three ThinkLabs One stethoscopes and a direct loopback of the input signal sent to the contact speaker. A UMC1820 Audio Interface was used to export the signals. The stethoscopes were placed on the sternum, directly below the contact speaker, and bilaterally on the posterior of the model aligned approximately with the fifth intercostal space. The stethoscopes and speaker were secured with elastic straps.
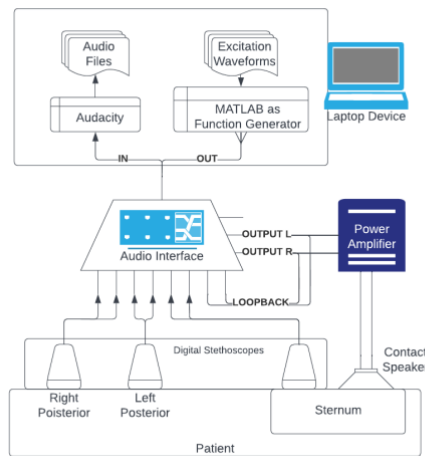
Figure 3-2: Diagram of experimental setup

3.3 Test Protocol

The model was considered at baseline with no air introduced into the anesthesia bags and an initial set of data recorded at baseline. Air was then introduced into the anesthesia bag to simulate a pneumothorax developing in increments of 500cc delivered by syringe through a three-way stopcock. Once the first side reached the maximum inflation of 2 L, simulating a massive unilateral tension pneumothorax, the second anesthesia bag was inflated in increments of 500cc until a bilateral tension pneumothorax was simulated. Each side was then decompressed one at a time by opening the stopcock, representing a needle decompression. Data was recorded between each decompression. Prior experimentation revealed that approximately 600cc of air remained in the anesthesia bags after passive

venting into the atmosphere. Thus, the remaining air was pumped out of the anesthesia bags and another data set collected. Lastly, due to previously observed hysteresis in the volume of the acoustic foam, the model was set to rest for 10 minutes to allow return to baseline and one final data set taken.

Table 3-3: Sample inflation plan for Trial 1, starting with the right side

Collection #	Right Inflation Volume (cc)	Left Inflation Volume (cc)
1	0	0
2	500	0
3	1000	0
4	1500	0
5	2000	0
6	2000	500
7	2000	1000
8	2000	1500
9	2000	2000
10	~600*	~600*
11	0**	~600*
12	0**	0**
13	0	0

* Anesthesia bag allowed to equilibrate to ambient pressure. Post testing revealed approximately 600cc of air still present.

** 0 cc of air left in anesthesia bags; however, hysteresis was noted in foam so another reading was taken 10 minutes later

The first two trials alternated which side was inflated first. After rough analysis, the third trial was modified to only take data from the sternum stethoscope, which produced the largest amplitude signal, and was held manually to simulate field conditions. At each increment of inflation, readings were taken both at the original position on the sternum and at the base of the sternum, approximately three ribs lower.

Data was also collected at the same locations on two healthy human volunteers to serve as a validation model for analysis.

3.4 Analysis Methods

From preliminary testing, four quantifiable characteristics of the response signal were identified. Resulting signals were visualized as a Fast Fourier Transform (FFT) and examined for the signal amplitude at different frequencies. First, the area under the FFT was found through numerical integration and used as a measure for the energy transmitted through the chest cavity. Second, the ratio of right and left stethoscopes was plotted as a function of total pneumothorax volume. Two frequency peaks were noted between 30-60 Hz and were analyzed for a local maximum and compared as a ratio as a function of pneumothorax volume. The third method calculated the damping coefficient of the decaying response to the transient impulse of the square wave. This coefficient was evaluated by least-squares fitting of a logarithmic decay on the peak-interpolated envelope of the impulse response for each instance of the 1Hz square wave. The fourth method located the crossover frequency of the response to the frequency sweep.


16
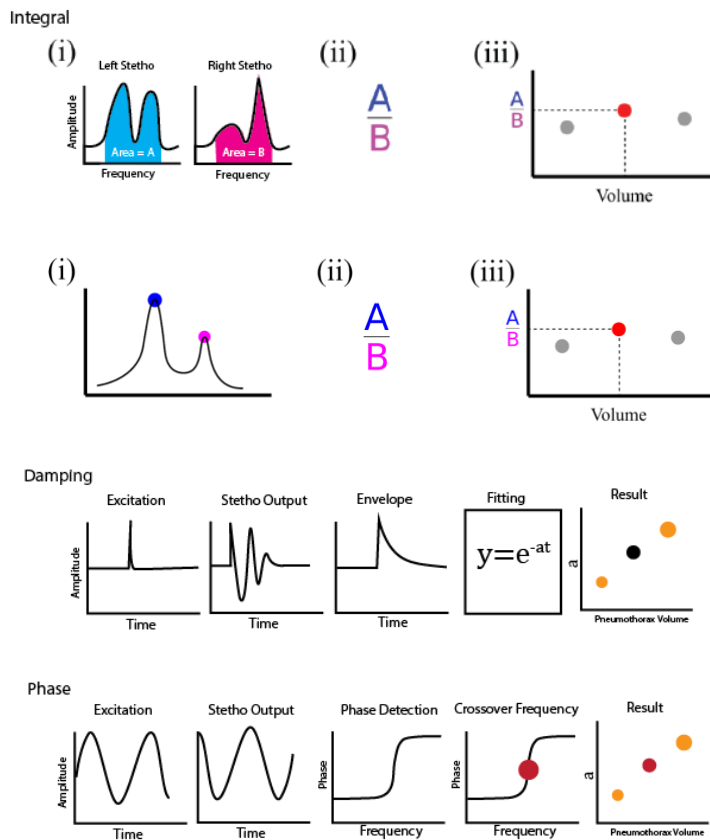
Figure 3-4: Simplified procedure for the 4 analyses done on the data in order to produce a pneumothorax metric. Row 1: pseudo-energy integral. Row 2: ratio of peaks. Row 3: damping coefficient. Row 4: crossover frequency.

3.5 Baseline Validation

Few to no data sets exist for the physio-mechanical properties and acoustics of the human thorax which makes validation of any phantom model difficult. We compared our phantom response data with data collected from two healthy humans using an identical sensor arrangement. The human data was compared with the "baseline" model data and the maximum bilateral pneumothorax data. The response was compared in both the frequency and time domains to assess whether the model response was comparable to the human body. Using a FFT and inspecting the frequency domain for both amplitude and phase lag, the model response was seen to follow the general shape of the human response. However, there was variation between each data set and the variance between both healthy humans was far greater than the two states of models. Within the time domain, examining the response to a single step input, a visual inspection validated approximately the same response between the model and a human. However, in this case, the variation between model states was far more significant than the variance between healthy humans.
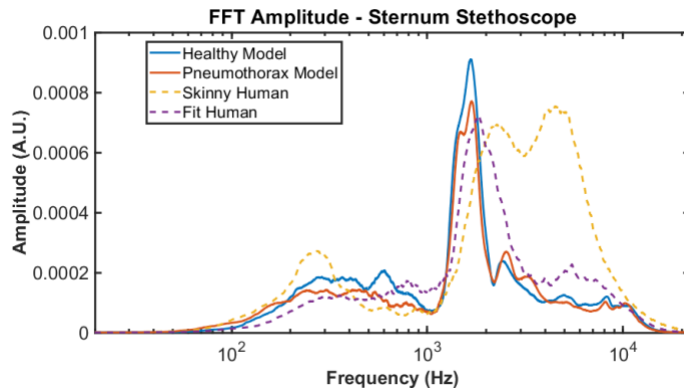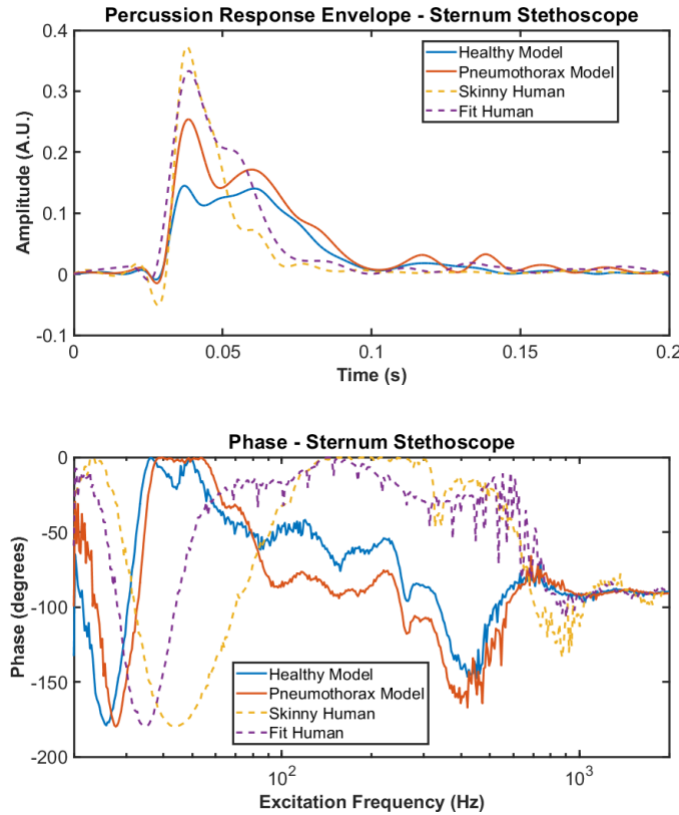
Figure 3-5: One run of data comparing humans and the model. Top: FFT output which is the input to the pseudo-energy integral and ratio of peaks method. Middle: envelope of the rectified impulse response, from which the damping coefficient was estimated. Bottom: phase lag between chirp excitation and response.

From this basic validation, the model had a characteristic response roughly resembling a human and thus was adequate to proceed with more detailed analysis. It should be noted however, that the model is unable to account for the significant natural variation between healthy humans and only presents a snapshot of a single manifestation of a human thorax. If statistically significant findings are present within the model data, further work will be needed to determine if the findings can be generalized to other sizes and shapes of bodies.

3.6 Results

Initial analysis after the first trial was promising, and showed correlations in all four characteristics examined, including a R^2 value of 0.801 comparing the ratio of peaks. While initial results were promising, additional trials failed to produce the same correlation. Trial three saw the trends

completely reversed in almost all categories compared. There was no discernable relation between the values measured and the volume of air introduced into the model.
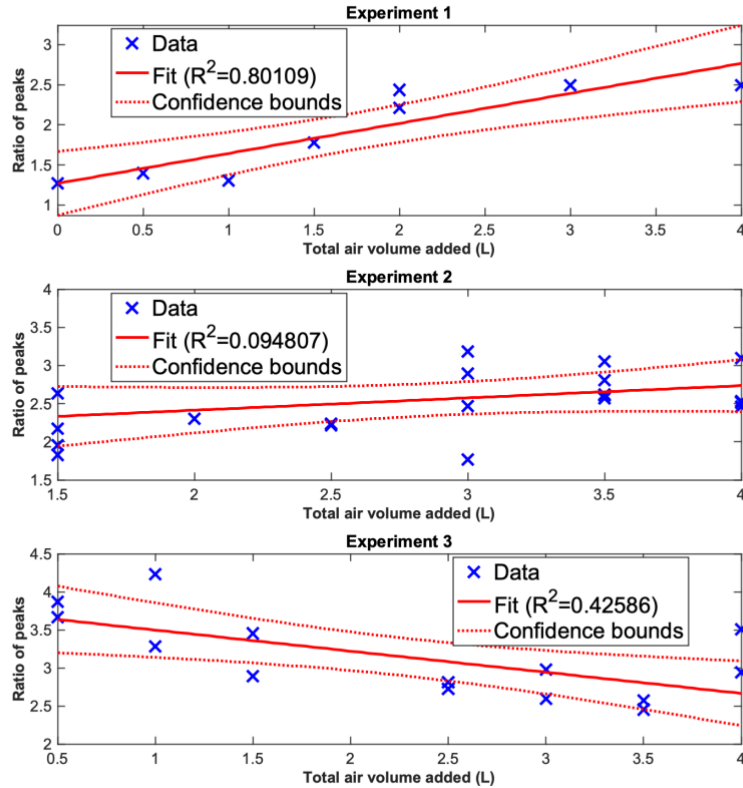
Figure 3.6: Result of ratio-of-peak analysis showing potential trends within individual trials but uncorrelated between multiple trials. The other analyses yield similar results. Please see the appendix for other results.

The results lacked repeatability both in initial values and correlation. Since the testing protocol was the same in each trial, but the model was re-set up before each trial, it can be inferred that there were additional uncontrolled variables that dominate the response characteristics. These variables must be identified and controlled to ensure reproducibility and to begin to assess for meaningful results within the data. Many of the uncontrolled factors may relate to the position and application of the stethoscopes on the phantom. While the same general anatomic location was used between trials, the exact spacing and orientation with regards to soft tissue versus bone was not controlled. Additionally, the normal force applied to the diaphragm of the stethoscopes varied by placement and orientation. Further testing showed

19

anecdotally the coupling between instrument and model changed drastically with different normal pressures.

Ultimately, our methods were inconclusive and unable to determine the presence or absence of a pneumothorax. The trials individually supported the likelihood of a correlated change of response characteristics due to introduction of pneumothorax, however no statistically significant or repeatable differences were observed. Further work to improve the fidelity of the phantom and validate the response characteristics against a human baseline is necessary to draw statistically significant conclusions from this testing protocol.

4. Future Works

Basic mathematical models of resonant cavities indicate that a change in response characteristics should accompany the introduction of a hemo/pneumothorax into the thoracic cavity. However, our limited attempt to prove that theory was unsuccessful and requires further refinement. Further efforts can be separated into two categories: improved mathematical modeling, and higher fidelity physical modeling.

4.1 Mathematical Modeling

In this experiment, basic acoustic principles were used to predict changes in resonant frequencies using broad assumptions and simplifications. Applying geometric analysis to the pleural space, like that performed in the construction of musical instruments and concert venues, could identify better predictions of resonant frequencies created by a large pneumothorax. Additionally, this study ignored the complexities of the rigid bone structure of the chest and any resonance inherent in those structures.

A full Finite Element (FE) simulation of the thoracic cavity would provide the best clarity of what responses could be expected for a given input. Studies evaluating the presence of hollows within watermelons determined that in their case, FE simulations of vibrational properties were an effective tool for studying the influence that position or direction of hollows has on the resonant frequency [14]. FE simulations could be performed using data from open-source 3D scanning methods such as MRI and CT scans.

4.2 Physical Modeling

The phantom model used in this study was constructed in a quick attempt to establish a test platform to collect data for analysis and was likely the source of unreliable data. It failed to account for the actual layering of flesh and muscle present within the human body. More care and detail in the selection of silicone rubber tissue analogs would lead to a phantom model that more accurately represents the intended characteristics.

Additionally, the structure of the lungs did not guarantee there was no air present in the pleural cavity at baseline and only relied on the inflation of a vessel to create the pneumothorax air bubble. The next iteration for this phantom will need more anatomically and physiologically accurate lungs that allow a baseline with lungs completely flush with the pleural walls. Either purpose-built analogs or commercially available synthetic organ replicas might suffice.

Lastly, the data collection setup was sensitive to a host of variables, including pressure, positioning, sensitivity settings, and filtering settings. A better constrained test rig would reduce the variation between trials and reduce signal noise.

5. Conclusion

The diagnosis of hemo and pneumothoraxes remains difficult without complex diagnostic imaging equipment. A method of detection was proposed using the characteristic response of the thorax to a known input and a model was fabricated to validate that method. Simple mathematical modeling and anecdotal evidence supported a change in resonant frequency and predicted a change in the response of the system, thus a mockup was created. A known signal was introduced to the thorax via a contact speaker placed on the sternum. The resulting sound waves were recorded with a series of electronic stethoscopes at predetermined locations around the body. The sound transmitted through the thorax was evaluated for changes indicating a pneumothorax might be present as progressively more air was introduced to the pleural space. The model response was compared to its own baseline and the same data collection scheme performed on two healthy adults. The results from multiple trials were analyzed and no discernible trend was found between the size or presence of a pneumothorax within any of the metrics identified for analysis.

While the attempt to validate the proposed method of identification was unsuccessful, the method itself remains supported by mathematical modeling and anecdotal evidence. This system was designed to prototype a diagnostic aid for emergency clinicians. As a result, the initial attempt was designed to be simple and accessible. Due to constraints of the project schedule and funding, creating a higher fidelity model for testing was impractical. A first principles model was fabricated in an attempt to verify the initial hypothesis. The model proved inaccurate and unreliable and would require additional development in flesh analogs and anatomically accurate lungs. Further studies can improve from the shortcomings of this investigation and continue to improve medical technology.

Future work could also include a dynamic model that adds the element of breathing through diaphragmatic contractions as well as optimization to work in austere emergency conditions often encountered by EMS. With future improvements and validation, this method could combine the elements required for generating the input, detecting the output, and analyzing the relationship into a single device to help guide medical professionals as they seek to treat potentially life-threatening emergencies from pneumothoraxes.

References

[1] Mowery, N. T., Gunter, O. L., Collier, B. R., Diaz, J. J. J., Haut, E., Hildreth, A., Holevar, M., Mayberry, J., and Streib, E., 2011, "Practice Management Guidelines for Management of Hemothorax and Occult Pneumothorax," J. Trauma Acute Care Surg., **70**(2), p. 510.

[2] American College of Surgeons and Committee on Trauma, 2018, *Advanced Trauma Life Support: Student Course Manual*.

[3] Leigh-Smith, S., and Harris, T., 2005, "Tension Pneumothorax—Time for a Re-Think?," Emerg. Med. J., **22**(1), p. 8.

[4] Wernick, B., Hon, H., Mubang, R., Cipriano, A., Hughes, R., Rankin, D., Evans, D., Burfeind, W., Hoey, B., Cipolla, J., Galwankar, S., Papadimos, T., Stawicki, S., and Firstenberg, M., 2015, "Complications of Needle Thoracostomy: A Comprehensive Clinical Review," Int. J. Crit. Illn. Inj. Sci., **5**(3), p. 160.

[5] Hacking, C., and Gorrochategui, M., 2008, "Pneumothorax," *Radiopaedia.Org*, Radiopaedia.org.

[6] Ravi, C., and McKnight, C. L., 2023, "Chest Tube," *StatPearls*, StatPearls Publishing, Treasure Island (FL).

[7] 2015, *Tension Pneumothorax and Needle Thoracostomy*, Larry Mellick.

[8] Netto, F. A. C. S., Shulman, H., Rizoli, S. B., Tremblay, L. N., Brenneman, F., and Tien, H., 2008, "Are Needle Decompressions for Tension Pneumothoraces Being Performed Appropriately for Appropriate Indications?," Am. J. Emerg. Med., **26**(5), pp. 597–602.

[9] Neeki, M. M., Cheung, C., Dong, F., Pham, N., Shafer, D., Neeki, A., Hajjafar, K., Borger, R., Woodward, B., and Tran, L., 2021, "Emergent Needle Thoracostomy in Prehospital Trauma Patients: A Review of Procedural Execution through Computed Tomography Scans," Trauma Surg. Amp Acute Care Open, **6**(1), p. e000752.

[10] 2016, "Parallel Tracks: The Rail Safety Story | Flight Safety Australia."

[11] Coffey, E., 2012, "Acoustic Resonance Testing," *2012 Future of Instrumentation International Workshop (FIIW) Proceedings*, pp. 1–2.

[12] Bono, R., and Schiefer, M., 2021, "Fundamentals of Resonant Accoustic Method."

[13] Diezma Iglesias, B., Ruiz-Altisent, M., and Orihuel, B., 2003, "ACOUSTIC IMPULSE RESPONSE FOR DETECTING HOLLOW HEART IN SEEDLESS WATERMELON," Acta Hortic., (599), pp. 249–256.

[14] Diezma Iglesias, B., Ruiz Altisent, M., and Jancsók, P., 2005, "Vibrational Analysis of Seedless Watermelons: Use in the Detection of Internal Hollows," Span. J. Agric. Res., **3**(1), p. 52.

[15] Ammari, H., Fitzpatrick, B., Gontier, D., Lee, H., and Zhang, H., 2018, "Minnaert Resonances for Acoustic Waves in Bubbly Media," Ann. Inst. Henri Poincaré C Anal. Non Linéaire, **35**(7), pp. 1975–1998.

[16] Garnett, E. S., Webber, C. E., Coates, G., Cockshott, W. P., Nahmias, C., and Lassen, N., 1977, "Lung Density: Clinical Method for Quantitation of Pulmonary Congestion and Edema.," Can. Med. Assoc. J., **116**(2), pp. 153–154.
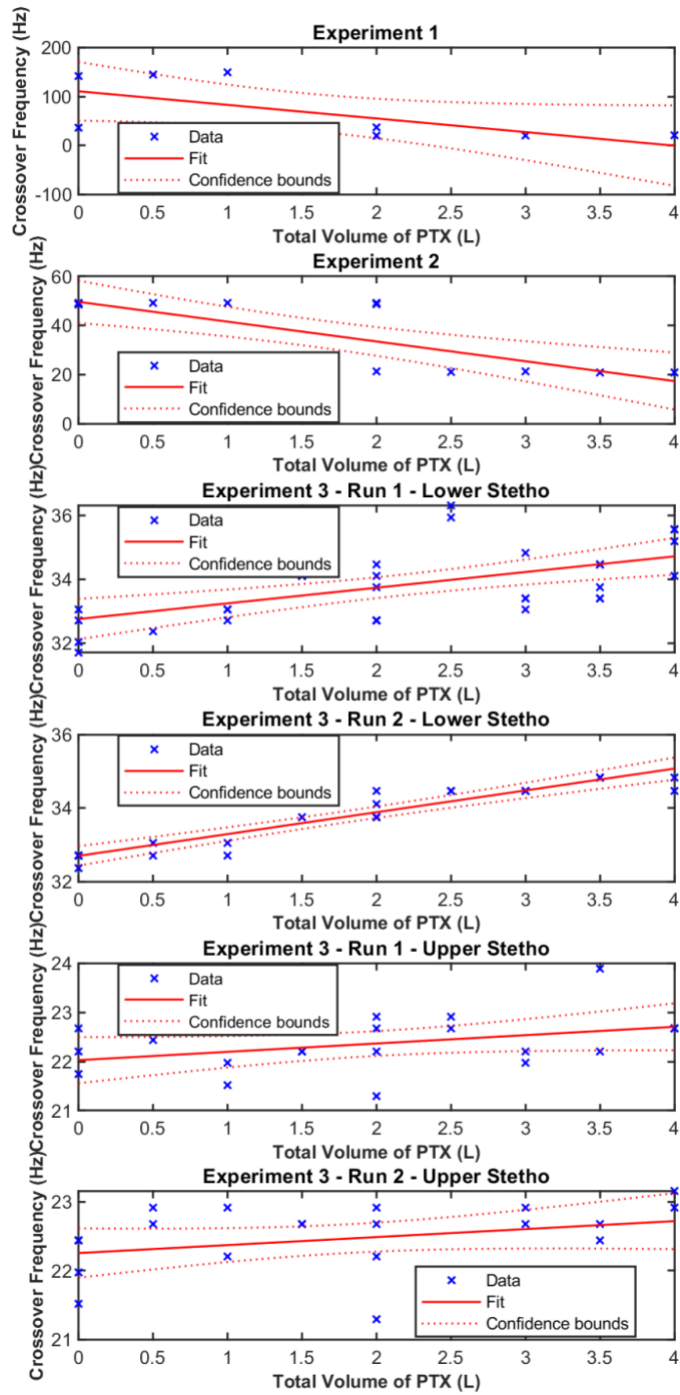
Appendix A: Additional Results
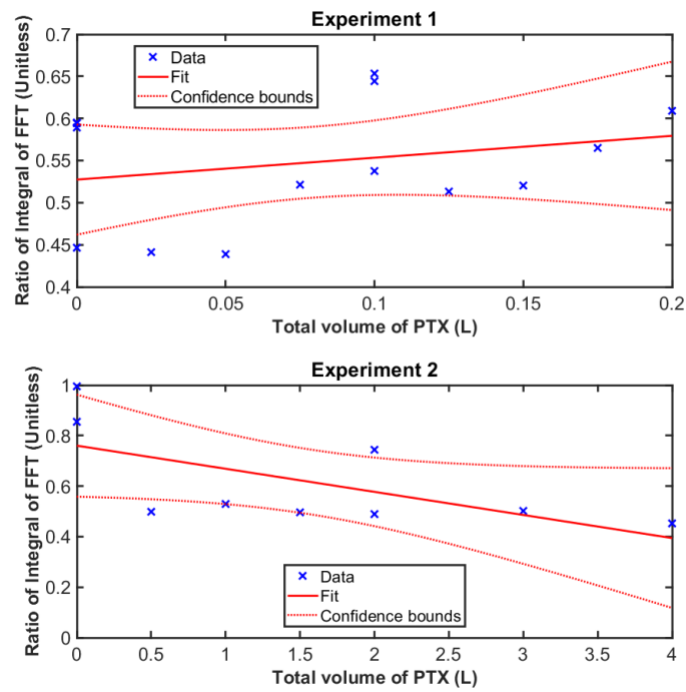
Figure A1: Results of FFT Integration analysis showing trends within each trial but uncorrelated between multiple experiments.
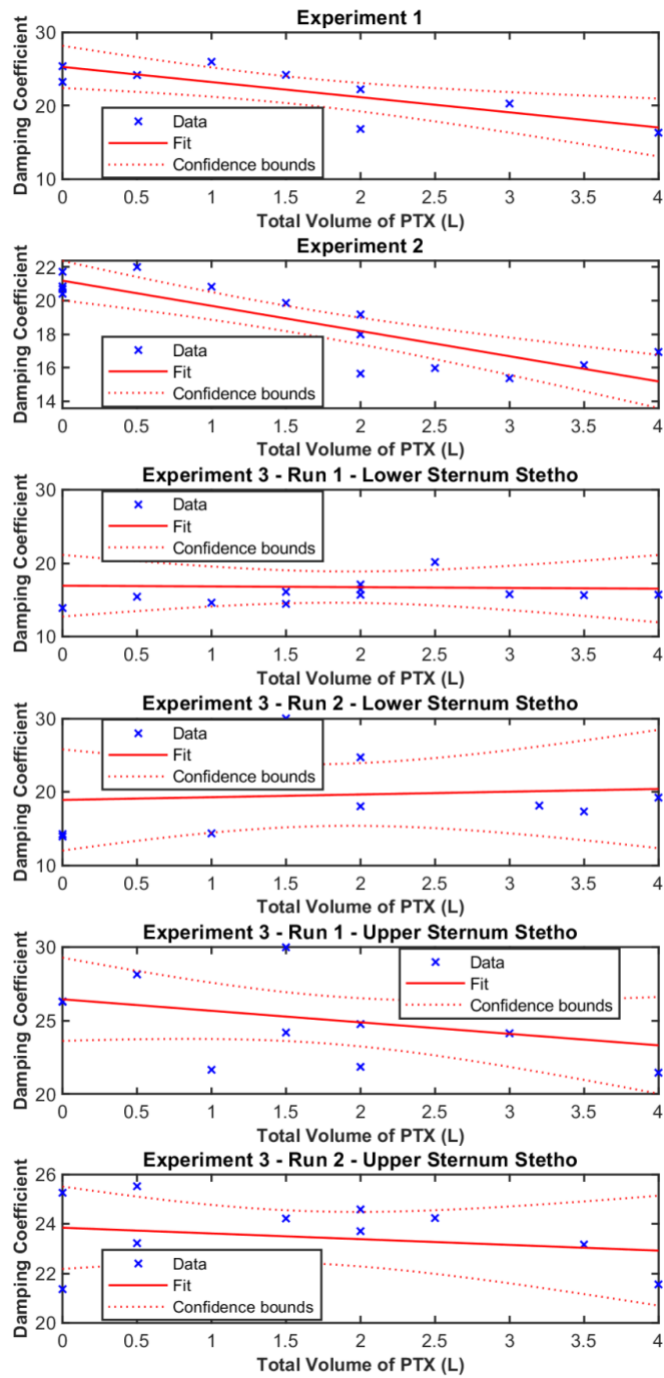
Figure A2: Results of damping coefficient analysis showing possible trends within each trial but uncorrelated between multiple experiments.

Figure A3: Results of crossover frequency analysis showing possible trends within each trial but uncorrelated between multiple experiments.